

## MULTI CLASS BRAIN TUMOR CLASSIFICATION OF MRI IMAGES USING HYBRID STRUCTURE DESCRIPTOR AND FUZZY LOGIC BASED RBF KERNEL SVM

A. JAYACHANDRAN AND R. DHANASEKARAN

**ABSTRACT.** Medical Image segmentation is to partition the image into a set of regions that are visually obvious and consistent with respect to some properties such as gray level, texture or color. Brain tumor classification is an imperative and difficult task in cancer radiotherapy. The objective of this research is to examine the use of pattern classification methods for distinguishing different types of brain tumors, such as primary gliomas from metastases, and also for grading of gliomas. Manual classification results look better because it involves human intelligence but the disadvantage is that the results may differ from one person to another person and takes long time. MRI image based automatic diagnosis method is used for early diagnosis and treatment of brain tumors. In this article, fully automatic, multi class brain tumor classification approach using hybrid structure descriptor and Fuzzy logic based Pair of RBF kernel support vector machine is developed. The method was applied to a population of 102 brain tumors histologically diagnosed as Meningioma (115), Metastasis (120), Gliomas grade II (65) and Gliomas grade II (70). Classification accuracy of proposed system in class 1(Meningioma) type tumor is 98.6%, class 2 (Metastasis) is 99.29%, class 3(Gliomas grade II) is 97.87% and class 4(Gliomas grade III) is 98.6%.

### 1. Introduction

Medical image segmentation has core importance to implement high level operations such as tissues recognition and classification. Image classification is one of the typical computer applications widely used in the medical field especially for abnormality detection in Magnetic Resonance brain images. Cancer has become a serious worldwide community health problem. According to the statistics given by the World Cancer Research Fund, yearly worldwide 12.7 million people are affected by cancer and in that nearly 50 percentage of them meet death. The annual death rate and affected rate due to cancer keeps rising. Brain tumor is a major social issue because it is extremely difficult to cure and also elevates both mental and economic problems to the patient. A good solution to this problem is early detection of tumor formation, which will help in better treatment [1]. Tumor in the brain is a cluster of anomalous cells growing up in the brain. The aggressive primary level brain tumors start mainly in the inside part of the brain. Metastatic tumor starts

---

Received: January 2013; Revised: April 2016; Accepted: December 2016

*Key words and phrases:* MRI, Classification, Fuzzy support vector machine, Feature selection, Texture, tumor class., Radial Basics Function (RBF).

as an inducing cancer cell somewhere in the other parts of human body and then migrates to the brain [3]. The objective of this study is to provide an automated tool that may assist in the imaging evaluation of brain neoplasms by determining the glioma grade and differentiating between different tissue types, such as primary neoplasms (gliomas) from secondary neoplasms (metastases). These issues are of critical clinical importance in making decisions regarding initial and evolving treatment strategies, and conventional MR imaging is often not adequate in providing answers [4]. Automated tools, if proven accurate, can ultimately be applied to (i) provide more reliable differentiation, especially when the neoplasm is heterogeneous and therefore cannot be adequately sampled by localized needle biopsy, (ii) avoid invasive procedures such as biopsy, especially in cases where the risks outweigh the benefits (iii) expedite or anticipate the diagnosis (histological examination is usually time consuming). Medical image classification is a pattern recognition technique in which different images are categorized into several groups based on some similarity measure. One of the significant applications is the tumor type identification in abnormal MRI brain images [5]. On the other hand, feature extraction is one of the most important methods for capturing visual content of an image. To facilitate decision making, such as pattern classification, feature extraction is used as the process to represent the raw image in its reduced form. This approach combines the intensity, texture, shape based features and classifies the tumor as white matter, gray matter, CSF, abnormal and normal area. The various methods such as multi texton histogram (MTH), principal component analysis (PCA) Texton co-occurrence matrix and linear discriminant analysis (LDA) are used for reducing the number of features. The MTH is a feature extractor and a descriptor to retrieve the content image which integrates the advantages of representing the attribute of the co-occurrence matrix using histograms. This descriptor analyzes the spatial correlation between neighboring color and edge orientation based on four special texton types [7, 8].

In recent times, a number of techniques have been developed for the segmentation of brain tissues from MR images. They are, classical pattern recognition techniques, rule-based systems, image analysis methods, crisp and fuzzy clustering procedures, feed-forward neural networks, fuzzy reasoning, geometric models to discover out lesion boundaries, related component analysis, deterministic annealing, atlas based techniques, and contouring approaches [9]. Considering the above techniques, Support Vector Machines (SVMs) are a popular tool for classification tasks due to their appealing generalization properties; this has led several groups to propose using SVMs for brain tumor segmentation. However, SVMs assume that data (here, individual voxels) is independently and identically distributed, which is not appropriate for tasks such as segmenting medical images. In particular, SVMs cannot consider dependencies in the labels of adjacent pixels. The basic idea is to find a hyper-plane which separates the  $d$ -dimensional data perfectly into its two classes. However, for example, data are often not linearly separable. SVMs introduce the notion of a kernel induced feature space which casts the data into a higher dimensional space where the data is separable [11, 14, 12]. The rest of the paper is organized as follows: proposed technique is feature extraction process is given in

section 2 and feature classification is given in section 3. The detailed experimental results and discussions are given in section 4. The severity analysis of real brain tumor images is given in section 5 and the conclusion is summarized in the conclusion section.

## 2. Hybrid Structure Descriptor

Feature extraction is to reduce the original data set by measuring certain properties, or features, that distinguish one input pattern from another pattern. The extracted feature is expected to provide the characteristics of the input type to the classifier by considering the description of the relevant properties of the image into a feature space. In this article, novel brain tumor classification algorithms have been developed to improve the performance of tumor classification accuracy in MRI images. The proposed method classifies MRI brain images into four different classes such as *Meningioma*, *Metastasis*, *Gliomas grade II* and *Gliomas grade III*. Initially the input image is passing through the anisotropic filter to eliminate the noise and enhance the image for further processing. Subsequently, the pre-processed image is segmented using region growing technique. After segmentation process, the features are extracted from the regions using hybrid structure descriptor and are given to the Fuzzy-HKSVM for training. In the final stage the image is classified four different tumor classes with the help of the trained Fuzzy kernel based support vector machine. The proposed method feature extraction consists of the following steps:

- Gridding
- Computation of Histogram vector of original image
- Computation of Histogram vector of orientation image
- Computation of Histogram vector of texton structure image
- Concatenation of the three vectors

**2.1. Gridding.** Normally, Gridding partitions the image into several smaller grid images. In this technique, original image is divided into 4, 18, and 24 grids. The grids are normally square in shape. Gridding results in smaller grids, so that the analysis can be performed easily.

**2.2. Computation of Histogram Vector  $H(V_1)$ .** In this technique, original image is divided into 4, 18, and 24 grids. Gridding results in smaller grids, so that the analysis can be performed easily. After the gridding process, the block count value is calculated for each intensity value of the original image from the intensity values 1 to 255. The resultant histogram vector is obtained from the original gridding image.

**2.3. Computation of Histogram Vector  $H(V_2)$ .** Texture is an important characteristic in image analysis and classification, and has attracted a lot of attention during the past decades. Texture classification is an important topic in the research areas of computer vision and pattern recognition. The proposed LTCoP is defined based on the first-order derivatives in eight directions as shown in Figure 1. The center pixel ( $g_c$ ) are defined as per equation (1).

$$\begin{aligned}\tilde{I}_{P,R}(g_i) &= I_{P,R}(g_i) - I_{P,R}(g_c); & i = 1, 2, \dots, P \\ \tilde{I}_{P,R+1}(g_i) &= I_{P,R+1}(g_i) - I_{P,R}(g_i) & i = 1, 2, \dots, P\end{aligned}\quad (1)$$

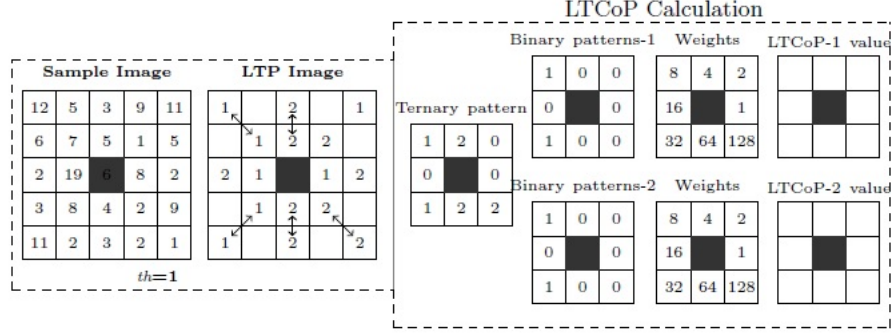


FIGURE 1. LTCoP Based Feature Extraction Calculation

After calculation of first-order derivatives, we code them based on the sign of derivative as per equation (2).

$$\begin{aligned} \tilde{I}_{P,R}^1(g_i) &= \tilde{f}_1(I_{P,R}(g_i)) \\ \tilde{I}_{P,R+1}^1(g_i) &= \tilde{f}_1(I_{P,R+1}(g_i)) \end{aligned} \quad (2)$$

The limited model among  $P$  neighborhoods,  $2P$  groups of binary models are doable, ensuing in feature vector length of  $2P$ . In arrange to decrease the computational cost the consistent models are used.

The co-occurrence value calculation process for LTCoP is defined as per equation (3).

$$\begin{aligned} \text{LTCoP} &= \begin{bmatrix} f_3(I_{P,R}^1(g_1), I_{P,R+1}^1(g_1)), \\ f_3(I_{P,R}^1(g_2), I_{P,R+1}^1(g_2)), \dots \\ \dots, f_3(I_{P,R}^1(g_P), I_{P,R+1}^1(g_P)) \end{bmatrix} \\ f_3(x, y) &= \begin{cases} 1 & \text{if } x = y = 1 \\ 2 & \text{if } x = y = 2 \\ 0 & \text{else} \end{cases} \end{aligned} \quad (3)$$

In this research work, those models which contain a smaller amount or equal amount of discontinuities in the globular binary depiction are referred to as the uniform models and left over models are non-uniform. Thus, the different uniform models for a specified inquiry image would be  $P(P-1)+2$  but destitute of revolving invariant. The revolving invariant LTCoP models can be defined by all eight directional models to the similar bin of histogram [6]. After the transformation of the original image, the histogram image is represented as per equation (4).

$$\begin{aligned} H_S(l) &= \frac{1}{N_1 \times N_2} \sum_{j=1}^{N_1} \sum_{k=1}^{N_2} f_4(PTN(j, k), l); \quad l \in [0, L-1] \\ f_4(x, y) &= \begin{cases} 1 & \text{if } x = y \\ 0 & \text{else} \end{cases} \end{aligned} \quad (4)$$

where,  $L$  means the number of bins and  $N_1 \times N_2$  means the dimension of the experimental image.

After LTCoP orientation process of original image, the partitioning process is applied, then, the block count value is calculated for each intensity value (1-255) on this image. The resultant vector  $H(V_2)$  is obtained from the orientation image.

**2.4. Computation of Histogram Vector  $H(V_3)$ .** The histogram vector computation process consists of two stages:

- Texton structure image formation.
- Block count value of texton structure image for each intensity value from 1 to 255.

*Texton structure image formation process:* Texton is one of the very important concepts for texture analysis; it was developed 20 years ago. It is a set pattern sharing a common property all over the image [10, 13]. In texton structure image formation, initially, detect the texton template using four special type of texton, then the texton structure map is extracted from the image using this texton templates, finally texton structure maps are fused to form the texton structure image for feature extraction is shown in Figure 2.

The texton structure map extraction process is a four step process as described below:

- (i) Divide the original image  $f(x, y)$  into  $3 \times 3$  blocks.
- (ii) Move the  $3 \times 3$  block horizontally and vertically from left to right and top to bottom throughout the original image  $f(x, y)$  with a step length of three pixels from the origin  $(0, 0)$ . Then, generate the texton structure map  $T_1(x, y)$ , where  $0 \leq x \leq M-1$ ,  $0 \leq y \leq N-1$ .
- (iii) Repeatedly doing the step (ii) from the origin  $(0, 1)$ ,  $(1, 0)$  and  $(1, 1)$  and generate the texton structure maps  $T_2(x, y)$ , where  $0 \leq x \leq M-1$ ,  $1 \leq y \leq N-1$ ,  $T_3(x, y)$ , where  $1 \leq x \leq M-1$ ,  $0 \leq y \leq N-1$  and  $T_4(x, y)$ , where  $1 \leq x \leq M-1$ ,  $1 \leq y \leq N-1$ , respectively.
- (iv) Generate the final texton structure map  $T(x, y)$  using the equation (5).

$$T(x, y) = \text{Max} \{T_1(x, y), T_2(x, y), T_3(x, y), T_4(x, y)\} \quad (5)$$

*Blocks count value of texton structure image:* In this system the values of a texton structure image  $T(x, y)$  are denoted as  $T(x, y) = w$ ,  $w \in \{0, 1, 2, \dots, N-1\}$ . In each  $3 \times 3$  block of  $T(x, y)$ ,  $P_0 = (x_0, y_0)$  denotes the center position on it and let  $T(P_0) = w_0$ ,  $P_i = (x_i, y_i)$  denotes the eight neighboring pixels to  $P_0$  and let  $T(P_i) = w_i$ ,  $i = 1, 2, 3, \dots, 8$ . Let  $N$  denotes the co-occurring number of two values  $w_0$  and  $w_i$ , and  $\bar{N}$  denotes the occurring number of values  $w_0$ . Moving the  $3 \times 3$  block from top to bottom and left to right throughout the texton structure image. The texton structure image is defined as per equation (6).

$$H(w_0) = \begin{cases} \frac{N\{T(P_0) = w_0 \wedge T(P_i) = w_i \mid |P_i - P_0| = 1\}}{8\bar{N}(T(P_0) = w_0)} \\ \text{where } w_0 = w_i, i \in \{1, 2, \dots, 8\} \end{cases} \quad (6)$$

After the formation of final texton structure image, then the block count value is calculated for each intensity value (1-255) on this image. The resultant vector  $H(V_3)$  is obtained from the texton structure image.

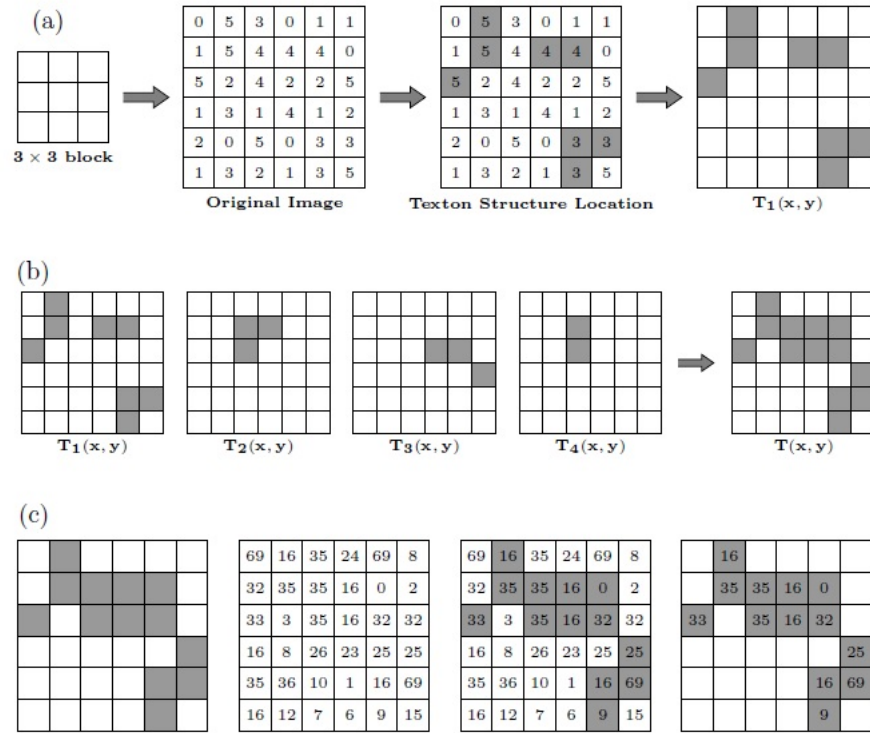


FIGURE 2. Texton Structure Image Extraction Process: (a) Texton Structure Map Extraction (b) Texton Structure Image Extraction Process (c) The Final Texton Structure Image Formation Process Using HSD

**2.5. Concatenated of the Three Feature Vectors.** Hence, total texture features  $H(V) = H(V_1) + H(V_2) + H(V_3)$  dimensional vector as the concluding image features in tumor classification.

### 3. Feature Classification

Supervised learning is a process in which the class labels of a set of instances are given and by applying a learning method, we build a classifier which can be used later in determining the class label of new instances. There are different ways of evaluating the performance of a classifier like using a separate test data, cross-validation, bootstrap sampling, and sub-sampling. In our proposed classification system, multiple kernels are combined to develop a new hybrid kernel that will improve the classification task of separating the training data [2, 16, 17, 18]. By introducing the hybrid kernel, SVMs gain flexibility in the choice of the form of the threshold, which need not be linear and even not to have the same functional form for all data, since its function is non-parametric and operates locally.

In most of the cases, an object is assigned to one of the several categories based on some of its characteristics in the real life situation. For instance, based on the outcome of several medical tests, it is mandatory to say whether the patient has a particular disease or not. In computer science, such situations are explained as classification issue. There are two phases in the support vector machine, namely, (1) Training phase and (2) Testing phase. In 2002, Fuzzy logic based SVM is developed by Wang et. al. [15], which is an effective supervised classifier and accurate learning technique. Here Fuzzy membership function is applied to each input data of SVM, the fuzzy training set is given in equation (7).

$$\{(x_i, y_i, s), i = 1, 2, \dots, n; x_i \in R^d; y_i \in \{1, -1\}; \lambda < s_i < 1\} \quad (7)$$

Here  $\lambda$  is a small positive number.

The optimal hyper plane problem of FSVM is defined in equation (8):

$$\begin{aligned} \min_{w, \zeta} \quad & \frac{1}{2} \|w\|^2 + C \sum_{i=1}^n f_i \varepsilon_i \\ \text{Subject to} \quad & y_i(w x_i + b) \geq 1 - \varepsilon_i \\ & \varepsilon_i \geq 0, i = 1, \dots, n \end{aligned} \quad (8)$$

where  $f_i (0 \leq f_i \leq 1)$  is the fuzzy membership function,  $f_i \varepsilon_i$  is a error of different weights and  $C$  is a constant.

The inputs to FSVM algorithm are the feature subset selected via HSD. In our technique, the brain has been classified into two classes: normal and abnormal brain. Then, a classification procedure continues to divide the abnormal brain into malignant and benign tumors and each subject is represented by a vector in all images. FSVM follows the structural risk minimization principle from the statistical learning theory. Its kernel is to control the practical risk and classification capacity in order to broaden the margin between the classes and reduce the true costs [19]. A Fuzzy support vector machine searches an optimal separating hyper-plane between members and non-members of a given class in a high dimension feature space.

The Lagrange multiplier function of FSVM is given in equation (9):

$$L(w, b, \xi, \beta) = \frac{1}{2} \|w\|^2 + C \sum_{i=1}^n f_i \xi_i - \sum_{i=1}^n \alpha_i (y_i (w z_i + b) - 1 + \xi_i) - \sum_{i=1}^n \beta_i \quad (9)$$

Which satisfies the following parameter condition:

$$\begin{aligned} w - \sum_{i=1}^n \alpha_i y_i z_i &= 0 \\ - \sum_{i=1}^n \alpha_i y_i &= 0 \\ f_i C - \alpha_i - \beta_i &= 0 \end{aligned}$$

Then the optimization problem is transferred, it is defined in equation (10):

$$\text{Max } W(\alpha) = \sum \alpha_i - \frac{1}{2} \sum \alpha_i \alpha_j y_i y_j k(x, y) \quad (10)$$

$$\text{Subject to } \begin{aligned} & \sum \alpha_i y_i = 0 \\ & 0 \leq \alpha_i \leq f_i C, \quad i = 1, 2, \dots, n \end{aligned}$$

Where the parameter  $\alpha_i$  can be solved by the sequential minimal optimization (SMO) quadratic programming approach.

We have analyzed the kernel equation from the existing work [14] and used them in the proposed work, namely, RBF and quadratic function.

*Radial basis function:* The support vector will be the centre of the RBF and will determine the area of influence. This support vector has the data space, it is given in equation (11):

$$K(x_i, x_j) = \exp\left(-\frac{\|x_i - x_j\|^2}{2\sigma^2}\right) \quad (11)$$

*Quadratic kernel function:* Polynomial kernels are of the form  $K(\vec{x}, \vec{z}) = (1 + \vec{x}^T \vec{z})^d$ . Where  $d = 1$ , a linear kernel and  $d = 2$ , a quadratic kernel are commonly used.

Let  $k_1$ (RBF) and  $k_2$ (Quadratic) be kernels over  $\Xi \times \Xi$ ,  $\Xi \subseteq R^P$  and  $k_3$  be a kernel over  $R^P \times R^P$ . Let function  $\varphi : \Xi \rightarrow R^P$ . The two kernels based formulations are represented in equations (12) and (13):

$$k(x, y) = k_1(x, y) + k_2(x, y) \text{ is a kernel} \quad (12)$$

$$k(x, y) = k_1(x, y)k_2(x, y) \text{ is a kernel} \quad (13)$$

Substitute the equations (12) and (13) in Lagrange multiplier equation (6) and get the proposed hybrid kernel. It is exposed in equation (14):

$$\begin{aligned} \text{Max: } W(\alpha) &= \sum \alpha - \frac{1}{2} \sum \alpha_i \alpha_j y_i y_j (k_1(x_i \cdot x_j) + k_2(x_i \cdot x_j)) \\ \text{Max: } W(\alpha) &= \sum \alpha - \frac{1}{2} \sum \alpha_i \alpha_j y_i y_j (k_1(x_i \cdot x_j)k_2(x_i \cdot x_j)) \end{aligned} \quad (14)$$

**Training and Testing Process:** To train the Fuzzy HKSVM classifier, we need some data features to recognize the brain tumor class. The data features, then train the classifier and the classifier will recognize the type of tumor. The data features, which we have chosen for training the classifier, are concatenated of the four feature vectors, such as blocks count value of the original image, orientation image, multi text on image and text on structure image for each intensity value (1-255). The Fuzzy HKSVM classifier then compares the values of the concatenated of the feature vectors with the various brain tumor classes. After comparison, the Fuzzy HKSVM classifier classifies the type of tumor, such as Meningioma, Glioma grade I, Glioma grade II and Metastasis.



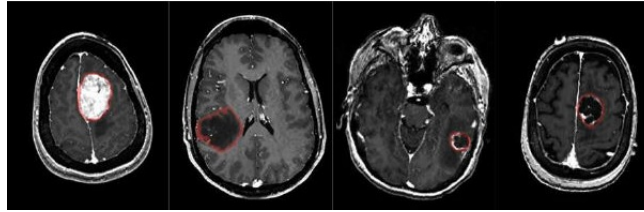


FIGURE 3. Sample Data Set: (a) Meningioma (b) Glioma Grade II, (c) Glioma Grade III (d) Metastasis

Tumor type	Training data	Testing data	Total no. of images
Meningioma	55	60	115
Metastasis	40	80	120
Gliomas grade II	30	35	65
Gliomas grade III	30	40	70
Total	155	215	370

TABLE 1. Experimental Image Dataset for Classification

#### 4. Experimental Materials and Results

**4.1. Materials.** The experimental image data set contains 452 brain MR images from four tumor types, namely Meningioma, Gliomas grade II, Gliomas grade III and Metastasis, that are collected from government medical college hospital, Tirunelveli, Tamilnadu, India. The sample experimental images are shown in Figure 3 and the different brain tumor types dataset is given in Table 1. In our proposed system, the brain image dataset is divided into two sets such as, (1) Training dataset, (2) Testing dataset. To segment the brain tumor images the training data set is used and to analyze the performance of the proposed technique the testing dataset is used.

**4.2. Experimental Methods.** This section describes the experimental results of the proposed classification method using brain MRI images with different types of tumors. In the proposed method, the brain image data set is divided into two sets such as training set and testing set. The classifiers are trained with the training images and the classification accuracy is calculated only with the testing images. In the testing phase, the testing dataset is given to the proposed technique to find the tumors in brain images and the obtained results are evaluated through evaluation metrics namely, sensitivity, specificity and accuracy [20], it is given in equation (15):

$$\begin{aligned}
 \text{Sensitivity} &= \frac{TP}{TP + FN} \\
 \text{Specificity} &= \frac{TN}{TN + FP} \\
 \text{Accuracy} &= \frac{TN + TP}{TN + TP + FN + FP}
 \end{aligned} \tag{15}$$

Class predicted	Ground Truth Class (Assigned by Radiologist)			
	Meningioma	Metastasis	Gliomas grade II	Gliomas grade III
Meningioma	57	1	2	0
Metastasis	3	75	1	1
Gliomas grade II	1	0	32	2
Gliomas grade III	2	0	0	38

TABLE 2. Confusion Matrix of HSD with Fuzzy-SVM

Where TP corresponds to True Positive, TN corresponds to True Negative, FP corresponds to False Positive and FN corresponds to False Negative. These parameters for a specific category, say, meningioma are as follows: TP is True Positive (an image of ‘meningioma’ type is categorized correctly to the same type), TN = True Negative (an image of ‘Non-meningioma’ type is categorized correctly as ‘Non-meningioma’ type), FP = False Positive (an image of ‘Non-meningioma’ type is categorized wrongly as ‘meningioma’ type) and FN is False Negative (an image of ‘meningioma’ type is categorized wrongly as ‘Non-meningioma’ type). ‘Non-meningioma’ actually corresponds to any of the three categories other than ‘meningioma’. Thus, ‘TP & TN’ corresponds to the correctly classified images and ‘FP & FN’ corresponds to the misclassified images.

The total of 370 brain masses were histologically diagnosed and graded based on World Health Organization (WHO) criteria as Metastasis (120), Meningiomas (115), Gliomas grade II (65) including astrocytomas, oligodendrogliomas, oligoastrocytomas, ependymomas and gliomatosis cerebri, Gliomas grade III (70) including anaplastic astrocytomas and (anaplastic) oligodendrogliomas.

The same feature sets are determined for all the categories by replacing ‘meningioma’ in the above definitions with other abnormal categories. Thus, different parameter values are obtained for each class and also for the different classifiers. These parameters are estimated from the confusion matrix which provides the details about the false and successful classification of images from all categories for each classifier. The confusion matrix of the HSD with Fuzzy-SVM is illustrated in Table 2 and the classification accuracy of the HSD with Fuzzy-SVM is given in Table 3.

In the Table 2, the row-wise elements correspond to the four categories and the column-wise elements correspond to the target class associated with that abnormal category. Hence, the number of images correctly classified (TP) under each category is determined by the diagonal elements of the matrix. The row-wise summation of elements for each category other than the diagonal elements corresponds to the ‘FN’ of that category. The column-wise summation of elements for each category other than the diagonal element corresponds to the ‘FP’ of that category. Similarly, ‘TN’ of the specific category is determined by summing the elements of the matrix other than the elements in the corresponding row and column of the specific category. For example, among the 60 meningioma testing images, 57 images have been successfully classified (TP) and the remaining 3 images (rst row-wise summation) have been misclassified to any of the non-meningioma categories (FN).

Class predicted	TP	TN	FP	FN	Sensitivity (%)	Specificity (%)	Accuracy (%)
Meningioma	57	149	6	3	91.93	96.13	95.81
Metastasis	75	134	1	5	93.75	99.26	97.21
Gliomas grade II	32	177	3	3	91.43	98.33	97.21
Gliomas grade III	38	172	3	2	95.00	98.29	97.64

TABLE 3. Performance Measure of HSD with Fuzzy-SVM

Class predicted	Ground Truth Class (Assigned by Radiologist)			
	Meningioma	Metastasis	Gliomas grade II	Gliomas grade III
Meningioma	59	0	1	0
Metastasis	1	78	1	0
Gliomas grade II	1	0	33	1
Gliomas grade III	0	1	1	38

TABLE 4. Confusion Matrix of Proposed Method  
(HSD with Fuzzy-HKSVM)

Class predicted	TP	TN	FP	FN	Sensitivity (%)	Specificity (%)	Accuracy (%)
Meningioma	59	153	2	1	98.33	98.70	98.60
Metastasis	78	134	1	2	97.50	99.26	98.60
Gliomas grade II	33	177	3	2	94.29	98.33	97.67
Gliomas grade III	38	174	1	2	95.00	99.43	98.60

TABLE 5. Performance Measure of Proposed Method  
(HSD with Fuzzy-HKSVM)

Similarly 6 images (rst column-wise summation) from the other three categories (non-meningioma) have been misclassified as meningioma category (FP). In the Table 3, the classification accuracy of HSD with Fuzzy-SVM in class 1(Meningioma) type tumor is 95.81%, class 2(Metastasis) is 97.21%, class 3(Gliomas grade II) is 97.217% and class 4(Gliomas grade III) is 97.64%. The miss classification rate of class 1(Meningioma) is high compared to the other three classes. The confusion matrix of the proposed method (HSD with Fuzzy-HKSVM) is illustrated in Table 4 and the classification accuracy is given in Table 5.

In the Table 5, the classification accuracy of Proposed method (HSD with Fuzzy-HKSVM) in class 1(Meningioma) type tumor is 98.6%, class 2(Metastasis) is 98.6%, class 3(Gliomas grade II) is 97.67% and class 4(Gliomas grade III) is 98.6%. The miss classification rate of class 3(Gliomas grade II) type tumor is highly compared

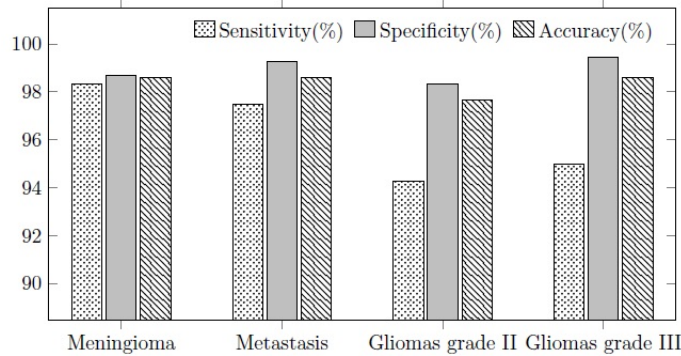


FIGURE 4. Multi Class Brain Tumor Classification Results of Proposed Method

with the other three classes. Based on the experimental results, our proposed method classification accuracy is highly compared with traditional method (HSD with FSVM). The obtained experimental results are plotted in Figure 4.

### 5. Severity Analysis

In severity analysis, five samples of brain tumor MR images are used for analysis. In this method, the pixel based similarity matching is performed between segmented tumor area by the proposed method and manually segmented area of the experimental tumor image. The Jacquard coefficient statistic method is used for comparing the similarity and diversity of sample sets, which is given in equation (16). The severity analysis of five different brain tumor image is shown in Table 6.

$$J(A, B) = \frac{A \cap B}{A \cup B} \quad (16)$$

Where  $A$  is the number of segmented pixels of the proposed method and  $B$  is the number of manually segmented pixels of the abnormal brain tumor image.

### 6. Conclusion

In this paper, a novel brain tumor classification method is developed, which includes segmentation, feature extraction, and multiclass classification of four classes of primary and secondary brain tumors. These tumors may have similar characteristics in their intensity and texture pattern; however, these tumors are different in their location, size, and shape. The proposed method is developed by multi model-texture features and fuzzy logic based RBF kernel support vector machine. Classification accuracy of proposed system in class 1(Meningioma) type tumor is 98.6%, class 2(Metastasis) is 99.29%, class 3(Gliomas grade II) is 97.87% and class 4(Gliomas grade III) is 98.6%. The developed methods for segmentation, feature extraction, and classification of brain tumors can be amalgamated to develop a CAD system. This system would be beneficial to radiologists for precise localization, diagnosis, and interpretation of brain tumors on MR images.

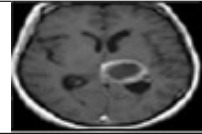
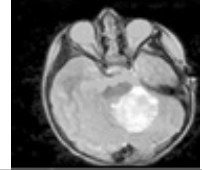
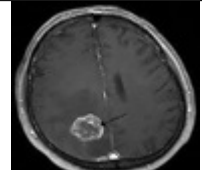
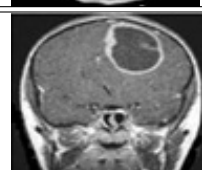
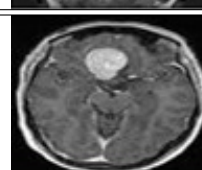
Experimental Images	Jacquard coefficient value (Pixel Count)	Tumor Type	Tumor Volume
	0.88	Anaplastic Astrocytoma, will grow faster.	$1.4321 \times 10^3$
	0.92	Anaplastic Astrocytoma, will grow faster, rarely spreads to other parts of the CNS.	$1.5060 \times 10^3$
	0.89	Metastase are a cancer that started in another part of the body and spread to the brain.	$1.2060 \times 10^3$
	0.94	Glioblastoma, most common type of primary brain tumor in adults.	$1.2060 \times 10^3$
	0.91	Meningioma, tumor that arises from a layer of tissue, grow on the surface of the brain.	$1.1610 \times 10^3$

TABLE 6. Severity Analysis of Multi Class Brain Tumor Images

## REFERENCES

- [1] S. Bauer S, L. P. Nolte and M. Reyes, *Fully automatic segmentation of brain tumor images using support vector machine classification in combination with hierarchical conditional random field regularization*, Med Image Comput Assist Interv., **14(3)** (2011), 354–361.
- [2] C. J. C. Burges., *A tutorial on support vector machines for pattern recognition*, Data Mining and Knowledge Discovery, **2** (1998), 121–167.
- [3] S. Chaplot , L. M. Patnai and N. R. Jagannathan , *Classification of magnetic resonance brain images using wavelets as input to support vector machine and neural network*, Biomedical Signal Processing and Control, **1(1)** (2006), 86–92.
- [4] J. Chunming Li, R. Huang, Z. Ding and J. Chris Gatenby, *A level set method for image segmentation in the presence of intensity in-homogeneities with application to MRI*, IEEE Trans Image Process, **20** (2011), 2007–2016.

- [5] R. Dhanasekaran and A. Jayachandran, *Brain tumor detection using fuzzy support vector machine classification based on a texton Co-occurrence matrix*, Journal of imaging Science and Technology, **57(1)** (2013), 10507-1–10507-7.
- [6] S. R. Dubey, S. K. Singh, and R. K. Singh, *Rotation and scale invariant hybrid image descriptor and retrieval*, Computers & Electrical Engineering, **46(8)** (2015), 288–302.
- [7] N. E. Ibrahim, S. Khalid and M. Manaf, *Seed-Based region growing (SBRG) vs adaptive network-based inference system (ANFIS) vs fuzzy c-means(FCM) - brain abnormalities segmentation*, World Acad. Sci. Eng. Technol., **68** (2010), 425–435.
- [8] A. Jayachandran and R. Dhanasekaran, *Automatic detection of brain tumor in magnetic resonance images using multi-texon histogram and support vector machinel*, International Journal of Imaging Systems and Technology, **23(2)** (2013), 97–103.
- [9] A. Jayachandran and R. Dhanasekaran, *Severity analysis of brain tumor in MRI images uses modified multi-texon structure descriptor and kernel- SVM*, The Arabian Journal of science and engineering, **39(10)** (2014), 7073–7086.
- [10] B. Julesz, *Texons—the elements of texture perception and their interactions*, Nature, **290** (1981), 91–97.
- [11] G. Kharmega Sundararaj and A. Jayachandran, *Abnormality segmentation and classification of multi-class brain tumor in MR images using fuzzy logic-based hybrid kernel SVM*, International journal of Fuzzy System, **17(3)** (2015), 434–443.
- [12] J. S. Lin, K. S. Cheng and C. W. Mao, *Segmentation of multispectral magnetic resonance image using penalized fuzzy competitive learning network*, Journal of Computers and Biomedical Research, **29(4)** (1996), 314–326.
- [13] G. H. Liu, L. Zhang, Yingkun Hou, Zuoyong Li and Jing-Yu Yang, *Image retrieval based on multi-texon histogram*, Pattern Recognition, **43(7)** (2010), 2380–2389.
- [14] C. L. P. Long-Chen, Philip Chen and L. U. Mingzhu, *A multiple-kernel fuzzy C-means algorithm for image segmentation*, IEEE Transactions On Systems, Man, and Cybernetics–Part B: Cybernetics, **41(5)** (2011), 1263–1274.
- [15] T. Wang and H. M. Chiang, *Fuzzy support vector machine for multi-class text categorization*, Information Processing and Management, **43** (2007), 914–929.
- [16] R. J. Young and E. A. Knopp, *Brain MRI: tumor evaluation*, Journal of Magnetic Resonance Imaging, **24** (2006), 709–724.
- [17] E. I. Zacharaki, S. Wang, S. Chawla, E. R. Melhem and C. Davatzikos, *Classification of brain tumor type and grade using MRI texture in a machine learning technique*, Magn. Reson. Med., **62** (2009), 1609–1618.
- [18] K. Zhang, H. X. Cao and H. Yan, *Application of support vector machines on network abnormal intrusion detection*, Application Research of Computers, **5** (2006), 98–100.
- [19] C. Zhu and T. Jiang, *Multi context fuzzy clustering for separation of brain tissues in magnetic resonance images*, Neuro Image, **18(3)** (2003), 685 –696.
- [20] W. Zhu, N. Zeng and N. Wang, *Sensitivity, specificity, accuracy, associated confidence interval and ROC analysis with practical SAS implementations*, In: Proceedings of the SAS Conference, NESUG 210, November 14–17, Baltimore, Maryland, 2010.

A. JAYACHANDRAN\*, DEPARTMENT OF CSE, PSN COLLEGE OF ENGINEERING AND TECHNOLOGY, TIRUNELVELI, INDIA  
*E-mail address:* [ajaya1675@gmail.com](mailto:ajaya1675@gmail.com)

R. DHANASEKARAN, DEPARTMENT OF EEE, SYED AMMAL ENGINEERING COLLEGE, RAMANATHAPURAM, INDIA  
*E-mail address:* [rdhanashekar@yahoo.com](mailto:rdhanashekar@yahoo.com)

\*CORRESPONDING AUTHOR

## MULTI CLASS BRAIN TUMOR CLASSIFICATION OF MRI IMAGES USING HYBRID STRUCTURE DESCRIPTOR AND FUZZY LOGIC BASED RBF KERNEL SVM

A. JAYACHANDRAN AND R. DHANASEKARAN

### دسته بندی تومور مغزی چند کلاسه بر اساس تصاویر ام.آر.آی با بکار بردن توصیف گر ساختاری مرکب و منطق فازی بر اساس RBF هسته SVM

چکیده . قطعه بندی تصویر طبی، افزاز تصویر به مجموعه ای از نواحی است که از نظر دیداری واضح و نسبت به برخی از خواص مانند سطح خاکستری، ساخت یا رنگ سازگار است. دسته بندی تومور مغزی در رادیو تراپی سرطان یک کار سخت و ضروری است. هدف از این تحقیق بررسی چگونگی استفاده از روش های دسته بندی الگو برای تشخیص انواع مختلف تومورهای مغزی، مانند تومور ابتدایی از طریق متاستاز و همچنین درجه بندی تومور می باشد. نتایج دسته بندی انجام شده دستی به نظر بهتر است، زیرا با هوش و فراست بشر در ارتباط است، اما اشکال آن است که ممکن است نتایج از شخصی به شخص دیگر متفاوت و نیاز به وقت بیشتری داشته باشد. تصویر ام.آر.آی بر اساس روش تشخیص اتوماتیک برای تشخیص های اولیه و معالجه تومورهای مغزی به کار برده شده است. در این مقاله با بکار بردن توصیف گر ساختاری مرکب و منطق فازی بر اساس جفت RBF هسته که ماشین بردار را حمایت می کند روش دسته بندی تومور مغزی چند کلاسه تمام اتوماتیک گسترش داده شده است. این روش در مورد تعداد ۱۰۲ تشخیص بافتی تومورهای مغزی مانند مننژیوم (۱۱۵)، متاستاز (۱۲۰)، تومور مغزی از درجه II (۶۵) و تومور مغزی درجه II (۷۰) به کار برده شد. دقت دسته بندی سیستم پیشنهادی در کلاس تومور نوع I (مننژیوم) ۹۸.۰۶٪، کلاس ۲ (متاستاز) ۹۹.۲۹٪، کلاس ۳ (تومور مغزی II) ۹۷.۸۷٪ و کلاس ۴ (تومور مغزی درجه III) ۹۸.۶٪ است.